Quantitative optical parameter determination in tissues using Diffuse Photon-Density Waves: The impact of measurement geometry and source modulation frequency

Thorsten Spott[ab], Tuan Pham[b], Lars O. Svaasand[a], Joshua B. Fishkin[b] and Bruce J. Tromberg[b]

[a]Dept. of Physical Electronics
Norwegian University of Science and Technology (NTNU)
N-7034 Trondheim
Norway

[b]Laser Microbeam and Medical Program (LAMMP)
Beckman Laser Institute and Medical Clinic
University of California
1002 Health Sciences Rd. East
Irvine, CA 92612
USA

ABSTRACT

The measurement of the propagation characteristics of Diffuse Photon-Density Waves (DPDW) is a viable path to determine the optical properties of tissue, i. e. the absorption and the reduced scattering coefficient. The technique allows to take measurements from bulk tissue, either by interstitial placement (infinite medium measurement) or superficial placement (semi-infinite medium measurement) of the source and detection fibers. Treatment of the tissue prior to measurement is unnecessary, such that changes to the structure of the tissue, and thus the optical properties, can be avoided. The optical properties can then be recovered by application of a diffusion model. When using a semi-infinite medium model, non-invasive *in vivo* measurements are feasible. While the theory is well established and verified by phantom measurements, the small amount of published data for biological tissue acquired by DPDW measurements suggests that there are still open practical problems, both concerning the measurement technique and the application of the diffusion model. In this study, we investigate the optimal choice of modulation frequencies for extracting a maximum amount of information on the scattering and absorption properties, examine different measurement setups, analyze how amplitude and phase data should be combined and compare the quality of infinite and semi-infinite medium measurements. The considerations are supported by experimental data, based on measurements from chicken and turkey breast muscle with modulation frequencies of up to 0.4 GHz.

Keywords: diffuse photon-density waves, diffusion theory, modulation frequency, optical properties, chicken breast muscle, turkey breast muscle

1. INTRODUCTION

The knowledge of macroscopic parameters describing the light transport properties of tissue is necessary in order to find the optimal light dose in therapeutic applications, and to gather information on the physiologic and structural status of the tissue for diagnostic purposes. The Boltzmann transport equation has proven generally suitable for the description of light propagation in tissue. As scattering is the dominant light interaction phenomenon in most tissues, application of the diffusion approximation to the transport equations is usually justified.[1] The optical properties are

Other author information:
T.S.: Email: thorsten@fysel.ntnu.no; Phone: ++47/73 59 44 16; Fax: ++47/73 59 14 41
T.P.: Email: tpham@bli.uci.edu; Phone: ++1/(949) 824-4713; Fax: ++1/(949) 824-8413
L.O.S.: Email: lars.svaasand@fysel.ntnu.no; Phone: ++47/73 59 44 21; Fax: ++47/73 59 14 41
J.B.F.: Email: jfishkin@bli.uci.edu; Phone: ++1/(949) 824-4713; Fax: ++1/(949) 824-8413
B.J.T.: Email: tromberg@bli.uci.edu; Phone: ++1/(949) 824-8705; Fax: ++1/(949) 824-8413

Part of the SPIE Conference on Optical Tomography and Spectroscopy of Tissue III
San Jose, California • January 1999 SPIE Vol. 3597 • 0277-786X/99/$10.00

then expressed in terms of the *absorption coefficient* μ_a, the *reduced scattering coefficient* μ_s' and the *index of refraction* n. The present study concentrates on the measurement of the former two; the determination of the refractive index has for example been treated by Bolin et al.[2]

The techniques in use for characterizing absorption and scattering of tissue can be classified into direct and indirect methods.[3,4] Direct methods determine the optical parameters directly, without requiring a model. Usually, light reflectance and transmission are measured with an integrating sphere technique, using thin tissue samples, such that multiple scattering interactions are unlikely. Most tissues need to be treated prior to measurement, either by cutting frozen material into very thin slices or by homogenizing and thereby transforming the tissue into a semi-liquid state. Unfortunately, processing the tissue often influences its optical properties. Indirect methods require a model to calculate the optical properties from transmission and reflectance measurements. As the model handles the description of multiple scattering interactions, larger sample sizes are possible and preparation of the tissue for measurement is usually unnecessary. Most biological tissues have high scattering albedos. Then, a valid approach to the modelling is given by the diffusion approximation to the Boltzmann transport equation.

Time- and frequency-resolved techniques are representatives of the group of indirect methods. They are related to each other by the Fourier transform. Patterson published original papers on both techniques,[5,6] followed by accounts of other investigators on different aspects of these methods, including experimental verification based on phantom tissue.[7–11] Using non-invasive measurements of the optical properties of breast tissue, efforts are under way to develop novel techniques for the diagnosis of breast carcinoma.[12,13] Due to the complex and to a wide degree unknown structure of breast tissue, a homogeneous medium model is applied. This approach has shown to be successful for detecting the relative changes in optical properties between normal and malignant tissue *in vivo*.

This study focuses on frequency-domain techniques, where high-frequency modulated light is injected into the tissue. Upon initial scattering, the light assumes isotropy and forms so-called *diffuse photon-density waves*, which become manifest in harmonic variations of the light intensity in the tissue. After measuring the attenuation and the phase shift of the density wave transmitted over a distance through the tissue, the optical properties are calculated by application of the P_1-approximation to the Boltzmann transport equation.

It seems that techniques using diffuse photon-density waves have not yet found widespread use for the quantitative determination of the optical properties of homogeneous biological tissue. Existing surveys are based on established methods.[14,15] In the present study, we develop guidelines for the application of frequency resolved measurements to the determination of the optical properties of bulk tissue. Section 2 presents the P_1-approximation to the Boltzmann transport equation and explains its application to infinite and semi-infinite medium measurements. The optimal choice of modulation frequencies is discussed, as well as the application of least-squares fitting routines to multi-frequency measurements of the amplitude and the phase. In Section 3 the theoretical considerations are applied to experimental data, measured from chicken and turkey breast muscle tissue. The last section discusses the results, in particular with respect to the differences between infinite and semi-infinite measurements.

2. THEORETICAL

The propagation of light in most scattering media is adequately described by the Boltzmann transport equation, which is an integro-differential equation in terms of the radiance L. In biological tissue the radiance is usually an almost isotropic quantity, and is well approximated by the sum of the isotropic *fluence rate* φ and the directional *flux* $\mathbf{j}$:

$$L(\mathbf{r},\mathbf{s}) = \frac{\varphi(\mathbf{r})}{4\pi} + \frac{3}{4\pi}\mathbf{j}(\mathbf{r})\cdot\mathbf{s} \tag{1}$$

where $\mathbf{s}$ is a unit vector pointing into the direction of interest. Upon substitution of (1) into the transport equation, the so-called P_1-approximation is found, which for a harmonic excitation of the light field with angular frequency ω can be written as:[16]

$$\nabla^2\varphi - \frac{\varphi}{\delta_c^2} = -\frac{q}{\zeta_c} \tag{2}$$

where the *complex penetration depth* δ_c is given by:

$$\delta_c = \left\{3\left[\mu_a\mu_{tr} - \frac{\omega^2}{c^2} + i\,\frac{\omega}{c}\,(\mu_{tr}+\mu_a)\right]\right\}^{-1/2} \tag{3}$$

and the *complex diffusion constant* by:

$$\zeta_c = \frac{\zeta_{DC}}{1 + i\omega\tau_{tr}} \tag{4}$$

ζ_{DC} is the steady-state value of the diffusion constant, defined by $\zeta_{DC} = (3\mu_{tr})^{-1}$, and τ_{tr} the *transport relaxation time*, given by $\tau_{tr} = (c\mu_{tr})^{-1}$. The source term q in (2) is for a point source with intensity P_0 given by $q(\mathbf{r}) = P_0\delta(\mathbf{r})$.

2.1. Infinite media

The Green's function of (2) in an infinitely extended, homogeneous medium is given by:[17]

$$\varphi(\mathbf{r},\omega) = \frac{P_0}{4\pi\zeta_c}\frac{1}{r}e^{-r/\delta_c} \tag{5}$$

For the following considerations, the complex penetration depth δ_c is more conveniently expressed by the sum of the attenuation k_r and the wavenumber (repetency) k_i:

$$\delta_c^{-1} = k_r + i\,k_i \tag{6}$$

such that:

$$k_r = \left[\frac{3}{2}\left(\mu_a\mu_{tr} - \frac{\omega^2}{c^2}\right)\right]^{1/2}\left[\left(1+\xi^2\right)^{1/2} + 1\right]^{1/2} \tag{7}$$

$$k_i = \left[\frac{3}{2}\left(\mu_a\mu_{tr} - \frac{\omega^2}{c^2}\right)\right]^{1/2}\left[\left(1+\xi^2\right)^{1/2} - 1\right]^{1/2} \tag{8}$$

where: $\xi = \frac{\omega}{c}\frac{\mu_a+\mu_{tr}}{\mu_a\mu_{tr}-\frac{\omega^2}{c^2}}$

Eq. (5) can then be restated as:

$$\varphi(\mathbf{r},\omega) = \frac{P_0}{4\pi\zeta_c}\frac{1}{r}e^{-k_r r}e^{-ik_i r} \tag{9}$$

The term $\exp(-k_r r)/r$ is a real quantity and describes how the amplitude of the variation of φ is attenuated with increasing distance from the source. The second exponential term is complex, and holds information about the phase shift.

At low frequencies, the attenuation k_r is to a high degree independent from the modulation frequency. This can be seen from the low frequency Taylor series expansion of k_r. Series expanding k_r with respect to $\omega\tau_a$, where $\tau_a = 1/c\mu_a$ is the *attenuation relaxation time*, assuming that $\omega\tau_a \ll 1$, gives:

$$k_r = \delta_{DC}^{-1}\left[1 + \frac{(\omega\tau_a)^2}{8}\right] + O(\omega\tau_a)^3 \qquad (\omega \ll \tau_a^{-1}) \tag{10}$$

The wavenumber k_i is approximately proportional to the modulation frequency, as long as the latter is low. This is evident from the series expansion of k_i:

$$k_i = \frac{1}{2}\,\delta_{DC}^{-1}\,\omega\tau_a + O(\omega\tau_a)^3 \qquad (\omega \ll \tau_a^{-1}) \tag{11}$$

Thus, at low modulation frequencies the phase velocity $v_p = \omega/k_i$ is to a wide degree independent from the modulation frequency. In the zero frequency limit, no information on the phase can be gained, and from the measurement of the amplitude, only the steady-state penetration depth $\delta_{DC} = (3\mu_a\mu_s')^{-1/2}$ can be determined.

An approximate expression for k_r and k_i at high modulation frequencies, such that $\omega\tau_a \gg 1$, but still $\omega^2\tau_a\tau_{tr} \ll 1$, is given by:

$$k_r \approx k_i \approx \sqrt{\frac{3\mu_s'\omega}{2c}} \qquad (\omega \gg \tau_a^{-1}, \omega^2 \ll (\tau_a\tau_{tr})^{-1}) \tag{12}$$

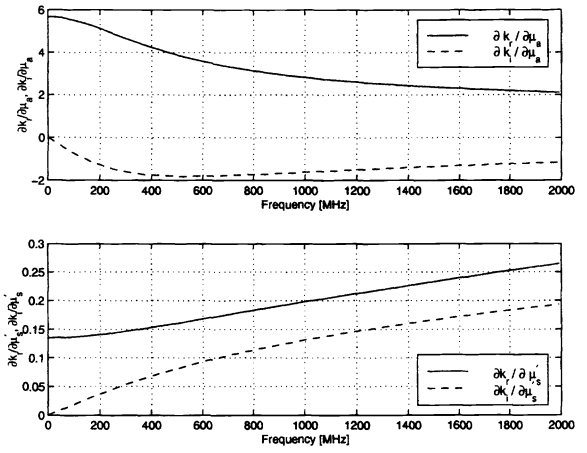

Figure 1. Sensitivity of k_r and k_i to changes in μ_a and μ_s' about $\mu_a = 10\,\mathrm{m}^{-1}$, $\mu_s' = 400\,\mathrm{m}^{-1}$, $n = 1.4$.

In this frequency range, attenuation and wavenumber tend to the same value and are widely independent from absorption.

The sensitivity of the attenuation coefficient and the wavenumber to changes in absorption and scattering, depending on the modulation frequency, are give in Fig. 1. The upper plot shows the graphs of the derivatives of k_r and k_i with respect to μ_a about $\mu_a = 10\,\mathrm{m}^{-1}$, and the lower plot the corresponding derivatives with respect to μ_s' about $\mu_s' = 400\,\mathrm{m}^{-1}$. It is apparent that the amplitude is most sensitive to changes in absorption in the zero frequency limit. Towards higher frequencies, sensitivity decreases. The derivative of k_i with respect to the absorption coefficient is always negative, indicating that an increase in absorption leads to a decrease in phase shift, or, in other words, to an increase in the phase velocity of the photon-density wave. In order to find the frequency at which k_i exhibits its maximum sensitivity to changes in μ_a, we observe that this maximum is reached at a frequency not too far beyond the absorption relaxation frequency $f_a = (2\pi\tau_a)^{-1}$, which is at 340 MHz in the example shown in Fig. 1, and far below the transport relaxation frequency $f_{tr} = (2\pi\tau_{tr})^{-1}$. Then $\omega^2 \ll (\tau_a\tau_{tr})^{-1}$ holds, and the diffusion approximation to the transport equation is applicable, i. e. the ω^2-terms in (8) can be neglected. Setting the second derivative of this approximate expression for k_i with respect to μ_a equal to zero reveals that the maximum sensitivity of k_i to changes in μ_a is reached at modulation frequencies of $f = \sqrt{3}f_a$. At higher frequencies, both the amplitude and the phase become increasingly insensitive to changes in absorption. This is contrasted by the sensitivity to changes in the reduced scattering coefficient, which increases monotonically with growing frequency. We thus find three frequency regions which are of particular interest for the determination of the optical properties:

1. The zero frequency limit. No phase information is available here, but sensitivity of the amplitude to changes in absorption is at its peak. Unfortunately, absorption and scattering are not separable in steady-state measurements; rather only the steady-state penetration depth δ_{DC} can be recovered. Low-frequency modulation of the light does not improve the situation, because the sensitivity of the amplitude to changes in absorption and scattering is largely indifferent to modulation frequency changes in this region. Steady-state measurements offer the advantage that they do not require specialized equipment, and they outperform high-frequency equipment easily in precision, as noise can be effectively suppressed by use of a lock-in amplifier.

2. The frequency around $f = \sqrt{3}\,f_a = \sqrt{3}(2\pi\tau_a)^{-1}$, i. e. where the phase sensitivity to changes in absorption is highest. Moreover, k_r and k_i are highly non-linear in this region, such that their separate determination from simultaneous measurements of phase and amplitude is possible.

3. Frequencies far beyond the absorption relaxation frequency. According to (12), the attenuation coefficient and the wavenumber are approximately equal in this regime. They are largely independent from μ_a and approximately proportional to the square root of the reduced scattering coefficient. The approximate equality of k_r and k_i implies that the intensity of the photon-density wave is attenuated by 27 dB on a path length corresponding to one wavelength. The wavelength behaves like $\lambda = 2\pi/k_i \propto \omega^{-1/2}$.

Assuming that the measured signal is proportional to the fluence rate (9), the attenuation k_r can be found from the ratio of the fluence rate at two distances from the source, r_1 and r_2:

$$k_r = \frac{\ln\left[\frac{r_1}{r_2}\frac{|\varphi(r_1)|}{|\varphi(r_2)|}\right]}{r_2 - r_1} \tag{13}$$

and the wavenumber k_i from the phase difference between the two measurements:

$$k_i = \frac{\phi(r_2) - \phi(r_1)}{r_2 - r_1} \tag{14}$$

The coefficients μ_a and μ_s' can then be recovered from (7) and (8).

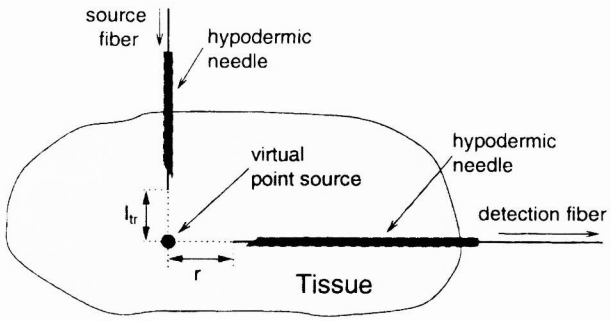

Figure 2. Experimental setup for infinite medium measurements.

Fig. 2 shows the setup for infinite medium measurements as used in the experiments. The source and the detection fiber are inserted into the tissue through hypodermic needles, perpendicular to each other, with the source fiber retracted by about one transport length l_{tr} from the extension of the path of the detection fiber. This distance corresponds approximately to one transport length $l_{tr} = \mu_{tr}^{-1}$, which is the average path length over which the directivity of a photon gets scrambled, i.e. over which the collimated source light beam assumes isotropy.[18] The diffuse photon-density wave can then be thought as originating from a virtual point source, placed in front of the detection fiber. The source-detector separation r is the distance between this point source and the detection fiber. The separation can be increased by retracting the detection fiber.

Unfortunately, the detected light signal is not proportional to the fluence rate alone in this setup. Since the detection fiber is collinear with the gradient of the fluence rate, an additional flux term is detected, following Fick's law. Accounting for this flux term in the model is often cumbersome, because the expressions become bulky, in particular when fitting routines such as the Levenberg-Marquardt algorithm are applied, which require the Jacobian matrix of the fitting quantities to be known. On the other hand, the flux, given by $\mathbf{j} = -\zeta_c \nabla\varphi$, consists of two terms in spherical geometries, one vanishing according to φ/r at larger distances, the other one being proportional to the fluence rate. When the measurements are taken sufficiently far away from the source, the measured intensity will be approximately proportional to the fluence rate, and the existence of a flux term can be neglected.

The assumption of proportionality between fluence rate and detected signal is true when the detection fiber is placed parallel to the source fiber. Unfortunately, this experimental setup is often prone to imprecision, as the detection fiber needs to be introduced independently at two different distances from the source fiber. Inserting the fiber is often connected with exerting mechanical stress on the tissue, and precise placement is difficult. Therefore this method often leads to rather large variations in the measurements. In fact, while extremely consistent results with parallely aligned fibers were obtained from liquid samples within this study, measurements of biological tissue were so inconsistent, that this fiber alignment was eventually abandoned.

2.2. Semi-infinite media

For these measurements, harmonically modulated light is transmitted as a collimated beam of ideally infinitely small diameter ("pencil-like beam") through the tissue surface. The optical properties can then be recovered from the

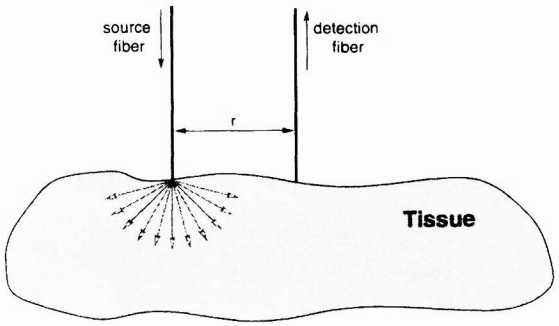

Figure 3. Semi-infinite medium measurement of optical tissue properties.

spatial distribution of the diffuse reflectance, i. e. from measurements of the light intensity on the tissue surface, away from the source. A sketch of the setup is depicted in Fig.3.

An approximate approach that gives a fairly accurate description of the conditions at the boundary and avoids bulky mathematical expressions was proposed by Haskell et al,[17] who unified the *partial-current boundary condition* and the *extrapolated boundary condition.* The measured signal at the surface is assumed to be proportional to the fluence rate:

$$\varphi_{AC} = \frac{P_0}{4\pi\zeta}\left[\frac{\exp(-r_a/\delta_c)}{r_a} - \frac{\exp(-r_b/\delta_c)}{r_b}\right] \tag{15}$$

where:
$$r_a = \left(l_{tr}^2 + r^2\right)^{1/2}$$
$$r_b = \left[(2z_b + l_{tr})^2 + r^2\right]^{1/2}$$
$$l_{tr} = \mu_{tr}^{-1}$$
$$z_b = \tfrac{2}{3}\tfrac{1+R_{eff}}{1-R_{eff}} l_{tr}$$

R_{eff} is given by an integral of the Fresnel reflection coefficient over 2π solid angle; its value depends on the refractive index n of the tissue. Haskell calculated $R_{eff} = 0.431$ for $n = 1.33$, and $R_{eff} = 0.493$ for $n = 1.4$.

A problem with the model for semi-infinite measurements when describing biological tissue is that the surface of many tissues is rather uneven, in contrast to the assumption of the boundary condition.

2.3. Extraction of optical properties from measurement data

2.3.1. Infinite medium measurement

In infinite geometries, the absorption and scattering coefficients are most conveniently determined by measuring the amplitude and phase of the light intensity at two distances from the point source. From (13) and (14), k_r and k_i are then calculated and μ_a and μ_s' can be determined.

Since only two variables are to be found, it is in theory sufficient to measure either both amplitude and phase at one modulation frequency, or either of them at two different frequencies. Tromberg et al[9] observed that the reliability of the recovered optical properties can be improved by multi-frequency calculations, because the influence of noise is reduced, and the knowledge of a bigger portion of the frequency response allows for an a-priori judgement of the quality of the measurements by comparison with the dispersion relations. Moreover, multi-frequency measurements offer more flexibility in choosing the frequency range such that the sensitivity considerations outlined above are accounted for. As modulation frequencies much greater than the absorption relaxation frequency $f_a = (2\pi\tau_a)^{-1}$ put a high demand on the measurement equipment, in many experimental settings the maximum frequency will lie around f_a. The problem does have a unique solution even at low frequencies; however, it is more difficult to separate μ_a from μ_s' due to low sensitivity to scattering changes in this regime. Under such circumstances it is advisable to acquire measurements over a broad frequency band and use a non-linear fitting algorithm, e.g. Marquardt-Levenberg,[19] in order to find an optimal fit for μ_a and μ_s' in the least-squares sense. The precision of the fitted variables can be further

improved by taking several measurements at every frequency, i. e. by sweeping several times over the frequency band, and determining the standard deviation of the measurement at every frequency. The optimal choice for μ_a and μ_s' can then be found by minimizing the expression:

$$\chi_\Gamma^2 = \sum_k \frac{[\Gamma_{\mathrm{mod}}(f_k;\mu_a,\mu_s') - \Gamma_{\mathrm{meas}}(f_k)]^2}{\sigma^2_{\Gamma(f_k)}} \tag{16}$$

where:

$\Gamma_{\mathrm{mod}}(f_k;\mu_a,\mu_s')$	value predicted by model, assuming μ_a and μ_s', at frequency f_k
$\Gamma_{\mathrm{meas}}(f_k)$	measured value at frequency f_k
$\sigma^2_\Gamma(f_k)$	variance of measurement at frequency f_k

In infinite medium measurements, Γ denotes k_r or k_i, according to which of the variables is fitted. If k_r and k_i are to be fitted simultaneously, (16) is applied to each of them, and the estimated values of μ_a and μ_s' are found from the minimum of $\chi^2 = \chi^2_{k_r} + \chi^2_{k_i}$. A priori the standard deviation is determined for the measurement quantities, i. e. the phase and the amplitude, not k_r and k_i. When the single measurement errors are assumed to be uncorrelated, the corresponding variance of the quantity to be fitted is given by:

$$\sigma^2_{\Gamma(f_k)} = \left[\frac{\partial\Gamma(f_k)}{\partial\eta(r_1)}\right]^2 \sigma^2_{\eta(r_1)} + \left[\frac{\partial\Gamma(f_k)}{\partial\eta(r_2)}\right]^2 \sigma^2_{\eta(r_2)} \tag{17}$$

where $\eta(r)$ is the measured quantity (here: amplitude A or phase ϕ) at distance r from the source. The variance of k_r and k_i is therefore given by:

$$\sigma^2_{k_r} = \frac{\frac{\sigma^2_{A(r_1)}}{A^2(r_1)} + \frac{\sigma^2_{A(r_2)}}{A^2(r_2)}}{(r_2 - r_1)^2} \tag{18}$$

$$\sigma^2_{k_i} = \frac{\sigma^2_{\phi(r_1)} + \sigma^2_{\phi(r_2)}}{(r_2 - r_1)^2} \tag{19}$$

The optimal choice of the fitting variable — amplitude, phase or both simultaneously — depends on how well the minimum of the χ^2 surface is defined. Figs. 4, 5 and 6 show the surface of χ^2 for the different fitting types. The signal was measured from a phantom, consisting of 0.3% intralipid and some nigrosine for additional absorption. The fitting was done with data taken at source-detector separations of 11 and 17 mm, with modulation frequencies ranging from 1 ... 400 MHz. When only one variable is fitted, the χ^2 surface forms a valley. The minimum of this valley is not very distinct and its position is likely to be affected by noisy data, leading to the estimation of incorrect optical properties. However, it is important to note that the valleys of the single fits stand at an angle relative to each other, such that a much better defined minimum is formed when both amplitude and phase data are fitted simultaneously. This is evident from Fig. 6. The optical properties estimated by simultaneous fitting were $\mu_a = 4.9\mathrm{m}^{-1}$ and $\mu_s' = 323\mathrm{m}^{-1}$.

2.3.2. Semi-infinite medium measurement

In the semi-infinite case, where the ratio of the measured amplitudes and the phase difference are fitted, the expressions for the standard deviation are:

$$\sigma_A^2 = \frac{1}{A^2(r_1)}\left[\frac{A^2(r_2)}{A^2(r_1)}\sigma^2_{A(r_1)} + \sigma^2_{A(r_2)}\right] \tag{20}$$

$$\sigma_\phi^2 = \sigma^2_{\phi(r_1)} + \sigma^2_{\phi(r_2)} \tag{21}$$

3. EXPERIMENTAL

The measurement system used in this study allowed us to investigate the propagation properties of diffuse photon-density waves with modulation frequencies up to 400 MHz, this upper frequency limit being imposed by the roll-off frequency of the avalanche photo-diode used to detect the light. On the source side, semiconductor lasers of four different wavelengths (674 nm, 803 nm, 849 nm and 894 nm) were intensity modulated by the signal originating from the frequency generator of a network analyzer (HP 8735C). From the laser diodes, the light was guided through optical fibers to a fiber-optic switch for wavelength selection, and then led through a 100 μm core graded index fiber to the tissue. On the detector side, the light was picked up either by a 550 μm core, 0.22 NA step index fiber

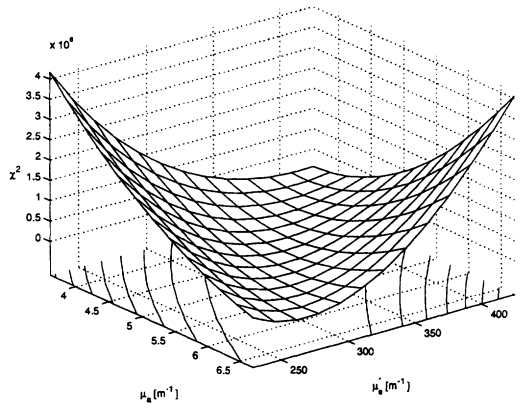

Figure 4. χ^2 vs. μ_a and μ_s' when fitting the attenuation k_r only. Data from: 0.3% intralipid solution, small amount of nigrosine added, infinite medium measurement, parallel fiber alignment, modulation frequencies: 1 . . . 400 MHz.

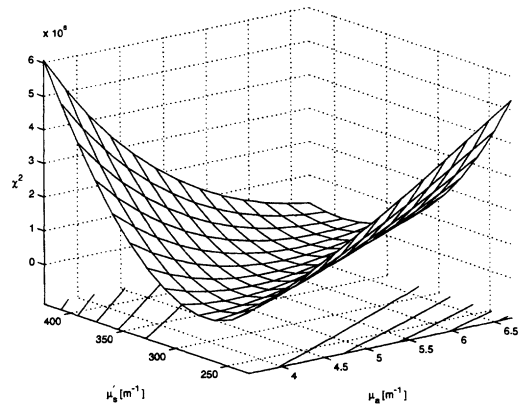

Figure 5. As Fig. 4, but fitting the wavenumber k_i only.

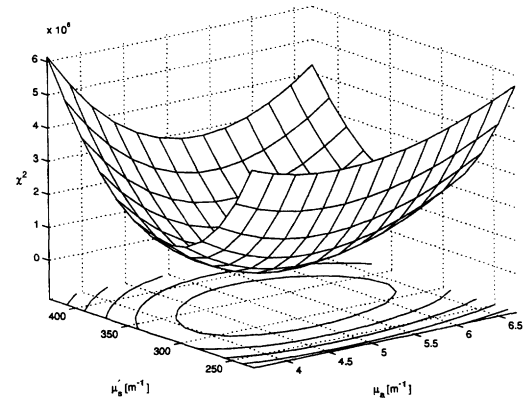

Figure 6. As Figs. 4 and 5, but fitting simultaneously k_r and k_i. Optical properties from this contour: $\mu_a = 4.9\,\mathrm{m}^{-1}$, $\mu_s' = 323\,\mathrm{m}^{-1}$.

(infinite medium measurements) or a 1 mm core, 0.39 NA step index fiber (semi-infinite medium measurements). Upon detection by the avalanche diode, the signal was fed back into the network analyzer and its amplitude and phase shift relative to the phase of the source signal determined.

Both chicken and turkey breast muscle of commercially available food quality were used as tissue samples. The model assumption of infinite and semi-infinite expansion of the tissue required the samples to have thicknesses corresponding to several penetration depths of the light. This was achieved by stacking 3–4 filets on top of each other, giving 6–9 cm thick tissue samples.

For the infinite medium measurements, the experimental setup followed the description in section 2.1 and Fig. 2. The transport length l_{tr} was estimated to be about 2.5 mm, and the source fiber retracted by this length relative to the line of the detection fiber. The range of distances between the virtual source and detector is at its lower end limited by the requirement to stay out of the region where there is still directed, non-isotropic radiation from the source, and where the contribution of the flux, which is not proportional to the fluence rate, is of importance. The maximum distance is given by signal strength and detector sensitivity. The smallest source-detector separation used in the measurements was 11 mm; this distance was then increased by gradually pulling the detection fiber out in steps of 2 mm, up to a distance of 21 mm. The modulation frequency was varied from 1 to 400 MHz, with 200 equidistant intermediate steps. From every pair of measurements being at least 4 mm apart, μ_a and μ_s' were calculated by fitting the amplitude data, the phase data or both simultaneously. From the obtained set of data, the mean value and the standard deviation were determined.

For semi-infinite measurements, the detection fiber was kept in a fixed position, barely touching the tissue surface, and the source fiber slightly above the tissue, such that it could be moved to distances between 9 and 19 mm relative to the detection fiber. The recorded data was evaluated analogously to the procedure described above. The positioning of the detector fiber just above the surface was a tradeoff. The assumption of the semi-infinite model that the tissue is bounded by air is violated when the detection fiber has close contact to the surface. As silica glass has a higher refractive index than tissue, the fiber then effectively acts as a sink for the light, which leads to a local perturbation of the light field in the tissue. On the other hand, the detectable signal becomes very weak when the fiber is kept distant from the tissue surface.

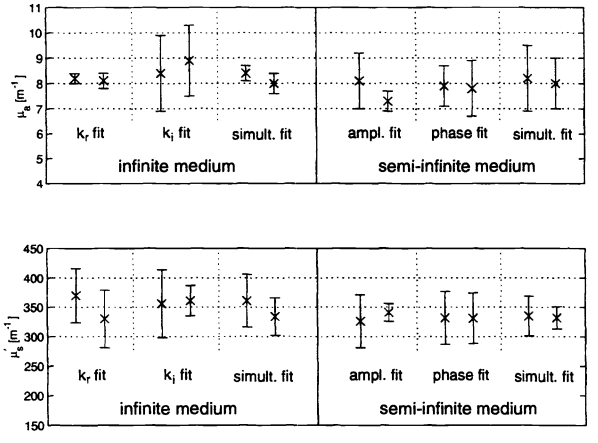

Figure 7. Optical properties of chicken breast muscle at 674 nm, two independent measurements: Comparison between infinite and semi-infinite medium measurements and amplitude, phase and simultaneous fit.

Results of measured optical properties using various fitting strategies are shown in Figs. 7 and 8. Phase fits alone were the least attractive option, as this led to rather inconsistent estimates and high standard deviations. The high consistency of μ_a when derived from infinite medium amplitude data reflects the observation made in section 2.1 that the sensitivity of the attenuation, i.e. k_r, to changes in absorption is particularly good in the frequency range chosen for the experiment. Sensitivity to changes in scattering is lower, and so is the consistency of the calculated μ_s'. Increasing the modulation frequency should alleviate this problem.

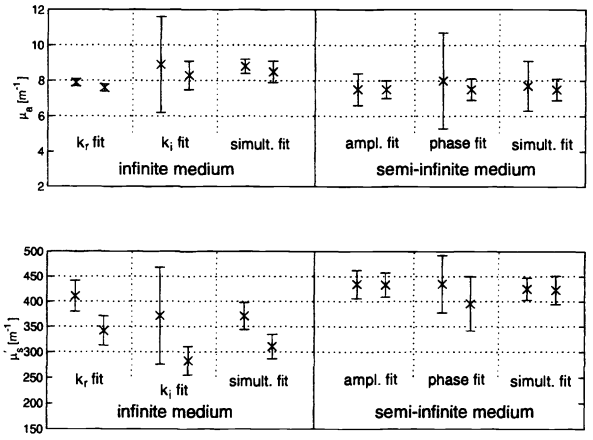

Figure 8. Optical properties of turkey breast muscle, two independent measurements: Comparison between infinite and semi-infinite medium measurements and amplitude, phase or simultaneous fit.

The semi-infinite medium measurements exhibit a higher consistency in the mean values of μ_a and μ_s' between the two measurement series, although the standard deviation is comparable to the infinite medium measurements. This problem is likely due to the unevenness of the tissue surface, leading to variations in light intensity transmitted through the surface of the tissue. The benefit of simultaneous fits for amplitude and phase is apparent: The calculated absorption and scattering coefficients clearly exhibit a better agreement than when amplitude or phase data are fitted alone.

Table 1 lists the numerical values of the absorption and reduced scattering coefficients, as well as the resulting steady-state penetration depths δ_{DC} of chicken and turkey breast muscle calculated from semi-infinite data and simultaneous phase/amplitude fits. It repeats the values shown graphically in Figs. 7 and 8, and gives in addition the optical properties at 803 nm, 849 nm and 894.

	Chicken breast muscle			Turkey breast muscle		
λ	δ_{DC}[mm]	μ_a[m^{-1}]	μ_s'[m^{-1}]	δ_{DC}[mm]	μ_a[m^{-1}]	μ_s'[m^{-1}]
674 nm	11.1 ± 0.6	8.2 ± 1.3	335 ± 34	10.3 ± 1.3	7.7 ± 1.4	425 ± 22
	11.5 ± 0.3	8.0 ± 1.0	332 ± 19	10.3 ± 0.5	7.5 ± 0.6	423 ± 28
803 nm	15.0 ± 1.7	5.6 ± 1.2	272 ± 26	13.8 ± 0.6	4.8 ± 0.4	368 ± 24
	15.6 ± 1.3	5.2 ± 1.0	269 ± 27	14.4 ± 1.2	4.1 ± 0.4	396 ± 30
849 nm	14.1 ± 1.1	6.6 ± 1.1	261 ± 39	13.0 ± 0.7	6.0 ± 0.6	329 ± 21
	14.2 ± 0.8	6.6 ± 1.0	253 ± 31	13.9 ± 0.3	5.0 ± 0.2	349 ± 19
894 nm	12.8 ± 0.8	8.4 ± 1.1	251 ± 37	12.2 ± 0.6	8.2 ± 0.6	274 ± 21
	12.9 ± 0.5	8.4 ± 1.3	243 ± 29	12.3 ± 0.6	7.7 ± 0.6	285 ± 29

Table 1. Optical properties of chicken and turkey breast muscle. Two semi-infinite medium measurements were taken independently at every wavelength.

4. DISCUSSION AND CONCLUSIONS

Whereas infinite medium model fits are computationally simpler, measurements are in practice more difficult to carry out. In order to limit the influence of the tissue boundaries on the measurement, the tissue sample should be sufficiently large so that its size corresponds to several penetration depths δ in any direction. The measured penetration depths of 10–15 mm suggest that the sample thickness should be at least of the order of 8 cm, such that several pieces of tissue have to be stacked together. This implies that the sample is rather heterogeneous, a particular problem for infinite medium measurements, since the exact location of the fiber tips inside the tissue stack can be

difficult to control. Moreover, stress is exercised on the tissue upon insertion of the fibers, with the danger of local optical property changes.

Another problem is the alignment of the fibers: A parallel alignment avoids picking up a flux term, but requires the detection fiber to be introduced several times into the sample. While this does not constitute a problem when measuring liquids, in solid tissue new holes must be poked for every measurement, producing mechanical stress in the tissue, and the fiber is prone to positioning inaccuracy. The parallel alignment resulted in fact in such a high degree of fluctuation in the measurements that it was abandonded during this study. A perpendicular alignment of the source and the detection fiber avoids the problem of multiple insertions, and the channel that the detection fiber is moved in for varying the source-detector separation does not seem to affect the measurements. A problem with the perpendicular alignment is the flux term. The error can be reduced by chosing the source-detector distance as large as possible, but this naturally leads to low signal levels.

Semi-infinite medium measurements avoid most of these experimental difficulties. As the model takes care of the boundary, the sample only needs to be half as thick as for infinite medium measurements. The area where the measurement is taken can be inspected, such that local inhomogeneities can to a certain degree be avoided. A restriction is that the surface of tissue tends to be rather uneven, which can make it difficult to do measurements at different distances under otherwise identical conditions. A theoretical problem of this measurement technique is the boundary condition, which is an approximation already for a smooth surface, and must be questionnable for the non-uniformly shaped boundaries of biological tissue. Practical experience has shown, however, that it describes the conditions sufficiently well, as long as the tissue surface seems comparatively even. Showing far more consistent values than the infinite medium measurements, semi-infinite measurements seem to be the technique of choice for determining the optical properties of bulk tissue.

An important aspect is the optimal choice of modulation frequencies. Most information can be gathered in the region of the absorption relaxation frequency, which for chicken/turkey muscle tissue means between 400 and 700 MHz. Whereas the sensitivity to changes in absorption diminishes towards higher frequencies, the opposite is true for the sensitivity towards changes in scattering. Low frequency data is comparatively easy to obtain, but modulation frequencies in the gigahertz range require specialized and expensive equipment equipment. A reasonable choice for the determination of the optical properties of muscle tissue seems therefore to combine measurements in the range from 100 MHz to 600 MHz with steady-state measurement data. Higher frequencies are beneficial for the accuracy of the reduced scattering coefficient. As the absorption relaxation frequency depends linearly on the absorption coefficient, low absorbing tissue can be well characterized with lower frequencies, whereas high absorbing tissue requires higher modulation frequencies. It should be noted that among muscle tissue, chicken and turkey breast have relatively low myoglobin content and hence relatively low absorption.

In any case, combining phase and amplitude data over a broad frequency region provides a reliable means for model function fits and accurate estimates of optical properties.

5. ACKNOWLEDGEMENTS

This investigation was performed with support from the NIH grants RR-01192 (Laser Microbeam and Medical Program) and GM-50958 (General Medical Sciences), the Office of Naval Research grant N00014-91-C-0134 (Medical Free Electron Laser Program) and the Department of Energy grant DE-FG03-91ER61227 (General Medical Sciences).

REFERENCES

1. A. Ishimaru, *Wave Propagation and Scattering in Random Media*, Adademic Press, 1978.
2. F. P. Bolin, L. E. Preuss, R. C. Taylor, and R. J. Ference, "Refractive index of some mammalian tissues using a fiber optic cladding method," *Appl. Opt.* **28**, pp. 2297–2303, June 1989.
3. B. C. Wilson, M. S. Patterson, and S. T. Flock, "Indirect *versus* direct techniques for the measurement of the optical properties of tissues," *Photochemistry and Photobiology* **46**(5), pp. 601–608, 1987.
4. B. C. Wilson, "Measurement of tissue optical properties: Methods and theories," in Welch and van Gemert,[20] ch. 8, pp. 233–274.
5. M. S. Patterson, B. Chance, and B. C. Wilson, "Time resolved reflectance and transmittance for the noninvasive measurement of tissue optical properties," *Appl. Opt.* **28**, pp. 2331–2336, June 1989.

6. M. S. Patterson, S. J. Madsen, J. D. Moulton, and B. C. Wilson, "Diffusion equation representation of photon migration in tissue," *IEEE MTT-S Digest* , pp. 905–912, 1991.
7. B. J. Tromberg, L. O. Svaasand, T.-T. Tsay, R. C. Haskell, and M. W. Berns, "Optical property measurements in turbid media using frequency domain photon migration," in *Future Trends in Biomedical Applications of Lasers*, pp. 52–58, SPIE, 1991.
8. J. B. Fishkin and E. Gratton, "Propagation of photon-density waves in strongly scattering media containing an absorbing semi-infinite plane bounded by a straight edge," *J. Opt. Soc. Am. A* **10**, pp. 127–140, Jan. 1993.
9. B. J. Tromberg, L. O. Svaasand, T.-T. Tsay, and R. C. Haskell, "Properties of photon density waves in multiple-scattering media," *Appl. Opt.* **32**, pp. 607–616, Feb. 1993.
10. L. O. Svaasand, B. J. Tromberg, R. C. Haskell, T.-T. Tsay, and M. W. Berns, "Tissue characterization and imaging using photon density waves," *Optical Engineering* **32**, pp. 258–266, Feb. 1993.
11. A. Kienle and M. S. Patterson, "Determination of the optical properties of semi-infinite turbid media from frequency-domain reflectance close to the source," *Phys. Med. Biol.* **42**, pp. 1801–1819, 1997.
12. H. Heusmann, J. Kölzer, and G. Mitic, "Characterization of female breasts *in vivo* by time resolved and spectroscopic measurements in near infrared spectroscopy," *J. Biomed. Opt.* **1**, pp. 425–434, Oct. 1996.
13. B. J. Tromberg, O. Coquoz, J. B. Fishkin, T. Pham, E. R. Anderson, J. Butler, M. Cahn, J. D. Gross, V. Venugopalan, and D. Pham, "Non-invasive measurements of breast tissue optical properties using frequency-domain photon migration," *Phil. Trans. R. Soc. Lond. B* **352**, pp. 661–668, 1997.
14. F. A. Duck, *Physical Properties of Tissue*, Academic Press, London, 1990.
15. W.-F. Cheong, "Summary of optical properties," in Welch and van Gemert,[20] ch. 8, Appendix, pp. 275–302.
16. L. O. Svaasand, T. Spott, J. B. Fishkin, T. Pham, B. J. Tromberg, and M. W. Berns, "Reflectance measurements of layered media with diffuse photon-density waves: A potential tool for evaluating deep burns and subcutaneous lesions," *Phys. Med. Biol.* **44**, pp. 801–813, March 1999.
17. R. C. Haskell, L. O. Svaasand, T.-T. Tsay, T.-C. Feng, M. S. McAdams, and B. J. Tromberg, "Boundary conditions for the diffusion equation in radiative transfer," *J. Opt. Soc. Am. A* **11**, pp. 2727–2741, Oct. 1994.
18. J. R. Lamarsh, *Introduction to Nuclear Reactor Theory*, Addion-Wesley, 1975.
19. P. R. Bevington, *Data reduction and error analysis for the physical sciences*, McGraw-Hill, New York, 2 ed., 1992.
20. A. J. Welch and M. J. C. van Gemert, eds., *Optical-Thermal Response of Laser-Irradiated Tissue*, Plenum Press, New York, 1995.